Comparative studies of structural and thermal gelation behaviours of soy, lentil and whey protein: a pH-dependency evaluation

Qi Tang[a,b], Yrjö H. Roos[b], Song Miao[a,c]*

[a] Teagasc Food Research Centre, Moorepark, Fermoy, Co. Cork, Ireland

[b] School of Food and Nutritional Sciences, University College Cork, Cork, Ireland

[c] China-Ireland International Cooperation Center for Food Material Sciences and Structure Design, Fujian Agriculture and Forestry University, Fuzhou, China

* Correspondence: song.miao@teagasc.ie; Tel.: +353-(0)-25-42468

Abstract

A growing global concern about human health, environment, and sustainable food supplies has motivated researchers to find new alternatives to dairy proteins. To investigate the effects of pH and protein varieties on the thermal gelation behaviors, plant protein (soy and lentil) and dairy protein (whey) were subjected to a variety of pH treatments. SDS-PAGE showed that only partial subunits of soy and lentil protein were involved in disulphide bonded aggregate formation regardless of pH, and that of whey protein was inhibited at acidic conditions and facilitated at higher pH. Both soy and lentil protein did not form self-standing gels at pH 5.0, while whey protein did, and all proteins displayed different morphologies as pH moved away from 5.0, from white, opaque, and heterogeneous to relatively transparent and homogeneous. Soy protein exhibited its optimal gel performance at pH 9.0 (storage modulus of 946.05 Pa) with the highest content of α-helix, intramolecular β-sheet, and intermolecular/aggregated β-sheet, while whey protein demonstrated its peak gel performance at pH 7.0 (storage modulus of 26271.90 Pa). Lentil protein displayed the best gel performance at pH 3.0 and was comparable to that of WPI (storage modulus of 5366.00 and 4965.00 Pa, respectively). These findings confirmed that LPI has the potential to substitute WPI and SPI in formulations of diversified food products in some specific pH systems. This work highlighted the importance of pH control to achieve desired gelation performance and offered valuable insights for selecting suitable protein alternatives in formulating plant-based food products.

Keywords: soy protein, lentil protein, whey protein, pH, thermal gelation property

1. Introduction

The by-product of cheese production, whey protein, which accounts for 20% of the total dairy protein, is widely used in dairy industry (e.g. gelling agent) due to its unique nutritional and functional properties (Dissanayake, Ramchandran, Piyadasa, & Vasiljevic, 2013). Whey proteins are globular proteins, and the major components of whey protein are β-lactoglobulin (β-Lg, ～18 kDa), and α-lactalbumin (α-La, ～14.4 kDa), which constitutes 50-55% and 20-25% of total whey protein, respectively. However, according Annex II of Regulation (EU) No 1169/2011, milk is identified as one of the fourteen major allergenic foods, among them, β-lactoglobulin is considered the most important allergic in whey protein (Kurpiewska, et al., 2019; Ng, et al., 2021). Aside from these, cholesterol issues, antibiotic residues, and lactose intolerance are also contributing factors to the surge demand of dairy protein alternatives (Vallath, Shanmugam, & Rawson, 2022).

Consequently, plant proteins are ideal candidates for sustainability-focused innovative ingredients in the food sector since they are health-promoting, environment-friendly, and cost-effective. Thus, the development of alternative plant proteins with excellent functional properties is urgent and meaningful. As one of the most widely used plant proteins in the food industry, soy has highest protein content (～ 40% seed protein) and protein digestibility-corrected amino acid score and protein efficiency ratio among all pulses (Vallath, et al., 2022). Nevertheless, the allergy issues mainly caused by its storage proteins as well as its beany flavor and off taste limits its application and allows new pulse protein options to emerge as a replacement of dairy protein. Lentil protein, a new emerging and underutilized protein has attracted the attention of researchers due to its excellent source of the essential amino acids, health-promoting properties (Samaranayaka, 2017). Furthermore, lentil protein shares similar major components to soy protein, which are 11S globulins (named glycinin and legumin) and 7S globulins (called β-conglycinin and vicilin), respectively.

Gelation, one of the most important properties in food products (e.g., cheese, yogurt, tofu, sausages) forms three-dimensional networks that allow entrapment of water, flavors, probiotic and food ingredients (Li & Zhao, 2018). The widely used method for protein gelation is thermal treatment, which involves denaturation, aggregation, and network formation. It is indeed evident that the process of thermal-induced gelation of plant globulins bears similarities to that of globular dairy proteins (Nicolai & Chassenieux, 2019). These globular proteins exhibit dense, well-defined, and rigid secondary and ternary structures in their native state, whereas these polypeptide chains undergo a loss of their rigid tertiary structure and become more mobile and flexible, facilitating the interaction of proteins to each other when subjected to heat treatment (Nicolai, 2019; Zheng, Regenstein, Zhou, & Wang, 2022). Two mechanisms are plausible during this process: (1) the buried cysteine residues that are not accessible in the native conformation are exposed and available, leading to intermolecular cross-links; (2) the physical phenomena of aggregation among protein molecules to counteract the exposed hydrophobic patches during heating that are typically buried within the protein native structure (Visschers & de Jongh, 2005).

The thermal-induced gel performance of proteins can be influenced by a variety of factors, including pH variations, which have intricate effect on the charge distribution and conformation of proteins, thus altering the strength and nature of the interactions involved in gel formation (e.g. hydrophobic interactions, hydrogen bonds and disulfide bridges) (Monahan, German, & Kinsella, 1995; Renkema, Lakemond, de Jongh, Gruppen, & van Vliet, 2000; Tanger, Müller, Andlinger, & Kulozik, 2022). For example, a shift from trimers (7S) to hexameric complexes (11S) of glycinin was observed at pH 3.8 (ionic strength = 0.03) to pH 7.6 (ionic strength = 0.5) (Lakemond, de Jongh, Hessing, Gruppen, & Voragen, 2000). Similarly, β-Lg existed primarily as dimers in aqueous solutions with pH 5.5 to 7.5 at room temperature, but dissociated into individual monomers as pH declined below 3.5 or exceeded

7.5, and associated into octamers at pH 3.7 to 5.1 (Mckenzie & Sawyer, 1967; Sittikijyothin, Sampaio, & Gonçalves, 2007). Additionally, pH shifts away from the isoelectric point (pI, pH 4-5), increasing net charge and solubility of proteins, resulting in the change from opaque (particulate type) to translucent (strand type) globular protein gels (Tang, Roos, & Miao, 2023b; Zheng, et al., 2022). However, different proteins may exhibit distinct response to pH conditions. For instance, the gel performance of whey protein was reported to be lowered at acidic conditions due to the hindered of disulphide reaction of β-lactoglobulin under acidic pH and promoted at alkaline conditions (Monahan, et al., 1995). Ge, et al. (2023) compared the thermal-induced gelation properties of legume proteins at pH 3.0 and 7.0 and found that the gel hardness of cowpea and mung bean protein was higher at pH 3.0, whereas that of soy and chickpea protein was higher at pH 7.0. The discrepancies in gel performance among pH and protein varieties resulted from the differences in the compositions of protein subunits and their secondary structures as well as intermolecular interactions and non-network protein content (Ge, et al., 2023). Despite many studies have conducted on the gelation properties of whey and soy protein individually (Dissanayake, et al., 2013; Kim, Varankovich, & Nickerson, 2016; Langton & Hermansson, 1992; Puppo & Anon, 1998; Renkema, et al., 2000), there is a notable absence of systematic investigations comparing the thermal-induced gelation properties of soy, lentil, and whey proteins under identical experimental conditions with varying pH levels. The limited knowledge and understanding of the pH-dependent behavior of these proteins pose challenges to unlock their potential application in food formulations with desired functional properties.

Herein, the present study investigated and characterized pH-dependent thermal gelation behaviors of soy, lentil, and whey protein, and explored the potential of substituting soy and whey protein with lentil protein. The structural, rheological, and mechanical properties of soy, lentil, and whey protein gels at different pH conditions were studied. Further, hierarchical

cluster analysis was employed to better understand the discrepancies in gel performance observed among proteins in response to different pH conditions. By investigating pH-dependent behavior of these proteins, we aimed to provide valuable insights into their potential application in food formulations and contribute to the development of protein-based products with enhanced functional properties.

2. Materials and methods

2.1. Materials

Soy (SPI, 89.96% ± 0.26 protein) and whey protein isolates (WPI, 86.93% ± 0.40 protein) were kindly provided by Archer Daniels Midland Company (Decatur, IL, USA) and Carbery Group Limited (Cork, Ireland), respectively. Red lentil protein flour donated by Fraunhofer (Munich, Germany) was further purified by alkaline extraction and acid precipitation to obtain lentil protein isolate (LPI, 89.07% ± 0.79 protein). Analytical grade chemicals were used in this study.

2.2. Sample preparation

Protein powders were dispersed in deionized water by stirring overnight, and then adjusted to different pH levels (pH 3.0, 5.0, 7.0, and 9.0) with a final protein concentration of 14% (*w/w*). The slurries were subsequently loaded into test tubes, sealed and heated in a water bath at 90 ℃ for 30 min. Finally, the obtained gels were immediately cooled and kept at 4 ℃ overnight before further analysis.

2.3. Gel characterization

2.3.1. Sol-gel phase diagram determination

The sol-gel phase diagram of different proteins was determined by their least gelation concentration (LGC) using a test-tube-inversion method. After mixing protein with deionized water overnight at 4 ℃, the suspensions were adjusted to pH 3.0, 5.0, 7.0, and 9.0 to make

suspensions with protein concentrations of 2.0 to 20.0% (*w/w*). The solutions were then transferred to sealed test tubes and incubated in a water bath at 90 ℃ for 30 min. The test tubes were then cooled in ice bath and stored at 4 ℃ overnight. LGC was defined as the lowest concentration at which the sample was stable and did not flow after the tube was inverted.

2.3.2. Dynamic rheological analysis

Dynamic modulus parameters (storage modulus (G′) and loss modulus (G″)) were determined by an AR2000ex rheometer (TA Instruments Ltd., Crawley, UK). The prepared solution (20 mL) with a protein concentration of 14% (*w/w)* at different pH (3.0, 5.0, 7.0, and 9.0) was loaded into the concentric cylinder geometry carefully with the recommended gap distance of 5920 μm. Peltier system (Viscotherm VT2, Phar Physica, Netherlands) was used to control temperature and a thin layer of paraffin oil was used to cover the geometry to prevent water evaporation. Temperature sweep measurements were performed within the linear viscoelastic region as the following protocols: equilibrated the sample solutions at 25 ℃ for 1 min, then heating the sample up to 90 ℃ at 1 ℃/min and then cooled to 25 ℃ at 1 ℃/min with angular frequency of 6.283 rad/s and strain of 1%. Then frequency sweep analysis was carried out on the formed gels with angular frequency from 0.628 to 62.83 rad/s at a fixed strain of 1% (linear viscoelastic region) at 25 ℃. The degree of angular frequency dependence was fitted using power law type equation:

$$\log G' = n' \log \omega + K' \quad (1)$$

$$\log G'' = n'' \log \omega + K'' \quad (2)$$

where G′ and G″ are the respective storage modulus and loss modulus, and K′ and K″ are the power law modulus constants of G′ and G″ (Pa· s^n), ω is the angular frequency, and n′ and n″ donate frequency dependence of G′ and G″ (dimensionless).

2.3.3. Texture profile analysis

The texture properties of protein gels were conducted by a TA-XT. Plus texture analyzer (Stable Micro System Ltd., Godalming, Surrey, UK) equipped with SMS P/75R probe. The gels were prepared in a 120 mL cylinders (diameter: 40 mm) following the procedure described in section 2.2. The prepared gels were compressed twice with the following parameters: load cell of 5 kg; pre-test speed of 2 mm/s; test speed of 1 mm/s; post-test speed of 3 mm/s; automatic trigger type; trigger force of 1 g; deformation of 30 %. Texture Exponent software (Stable Micro Systems) was used to calculate the textural attributes of gels.

2.3.4. Gel water retention

The water holding capacity (WHC) of gels were measured by applying the procedure from Tang, Roos, and Miao (2023a) with minor modifications. Protein slurries (10 g, 14% *w/w*) were loaded into 50 mL centrifuge tubes and heated at 90 ℃ for 30 min after mixing thoroughly. Next, the gel samples (M_S) were immediately cooled and kept at 4 ℃ overnight, followed by centrifugation at 8000× g for 20 min at 4 ℃. The gels (M_R) were reweighted after inverting the centrifuge tube to discard the isolated water. WHC was calculated as the following equation:

$$WHC = \frac{MR}{Ms} \times 100\% \quad (3)$$

2.4. Physicochemical and structural fingerprinting

2.4.1. Gel electrophoresis

Sodium dodecyl sulfide-polyacrylamide gel electrophoresis (SDS-PAGE) of thermal-induced SPI, LPI, and WPI gels were conducted using 12% MINI-Protein® TGX™ precast polyacrylamide gels (Bio-Rad Laboratories, Ireland) under non-reducing/reducing conditions (dithiothreitol, DTT). Protein gels were mixed with NuPAGE LDS sample buffer (4X, Invitrogen, Thermo Fisher Scientific, Cork, Ireland) and reducing agent (10X, Invitrogen,

Thermo Fisher Scientific, Cork, Ireland) or Milli Q water and centrifuged at 8000× *g* for 10 min before heating at 70 ℃ for 10 min. Afterwards, 20 μL protein samples and 10 μL PageRuler Unstained Protein Ladder #26616 (Thermo Fisher Scientific Inc., Ireland) were applied into the commercial gels separately, and subjected to electrophoresis using Mini-PROTEAN Tetra System (Bio-Rad Laboratories, Ireland) with a voltage of 120 V for 1h. The gels were stained with ready blue protein gel stain (EMD Millipore Corporation, Merck KGaA, Darmstadt, Germany) after electrophoresis. The gels were scanned using Epson Perfection V850 Pro scanner.

2.4.2. Fourier transform infrared (FTIR) spectral profiling

The obtained gels were freeze-dried, and infrared spectra of all samples were measured using the method described by Tang, et al. (2023b). Attenuated total reflectance accessory (PIKE Technology, Madison, WI, USA) mounted in FTIR spectroscopy (Bruker Tensor 27, Bruker Optik GmbH, Ettlingen, Germany) were used for FTIR spectra analysis. The spectra of each sample were recorded in a wavenumber range 4000-900 cm^{-1} and 120 scans and accumulated at 4 cm^{-1} resolutions at room temperature. Spectra of the amide I band (1700-1600 cm^{-1}) were analyzed using Spectragryph software (v.1.2.16.1, Oberstdorf, Germany) by performing baseline correction, second derivative, and smoothing. The secondary structure of these samples were then determined according to method described by Markoska, Daniloski, Vasiljevic, and Huppertz (2021). The deconvoluted sub-peaks can be assigned as follows: 1614-1600 cm^{-1} (side chain), 1637-1615 cm^{-1} (intramolecular β-sheet), 1645-1638 cm^{-1} (random coil), 1664-1646 cm^{-1} (α-helix), 1665-1681 cm^{-1} (β-turn), and 1700-1682 cm^{-1} (intermolecular/aggregated β-sheet) (Daniloski, McCarthy, Auldist, & Vasiljevic, 2022).

2.4.3. Colour determination

The colour properties of different gels were determined by Chroma meter (CR-400, Konica Minolta Sensing, Inc., Osaka, Japan). L^* (Lightness, white to black), a^* (redness to greenness) and b^* (yellowness to blueness) were used to indicate the colour of gels (Santana, Huda, & Yang, 2015). Whiteness index (*WI*) was calculated as following equation:

$$WI = 100 - \sqrt{(100 - L^*)^2 + a^{*2} + b^{*2}} \quad (4)$$

2.4.4. Confocal laser scanning microscopy (CLSM)

The microstructures features of gels formed at different pH conditions were observed at ambient temperature using a Leica TCS SP5 microscope (Leica Microsystems CMS GmbH, Germany) (Pereira, Bennett, Hemar, & Campanella, 2001). Rhodamine B (0.1%, *w/v*, in Milli Q water) was selected as fluorescent dye for labelling protein phase. The sliced and stained samples were inserted between a glass slide and a coverslip with an oil drop on it. HCX PL APO lambda blue 63x 1.4 OIL lens was used as the objective lens to observe the microstructural of gels. Rhodamine B was excited at 488nm using argon laser and the corresponding emission filter was set at 651-615 nm. Leica LAS AV software (v 2.7.3.9723; Leica Microsystems CMS GmbH) was used to acquire digital images 1,024 × 1,024 pixels in size.

2.5. Data analysis

Data were expressed as mean ± standard deviation. The mean multiple comparison test was performed using one-way analysis of variance (ANOVA) with the level of significance differences being $p \leq 0.05$ (Duncan's test) by SPSS 20.0 software (Chicago, USA). Hierarchical cluster analysis (HCA) and figures were performed using Origin 2021 software (Origin Lab, Corporation, Northampton, MA, USA).

3. Results and discussion

3.1. Gelation performance analysis

3.1.1. Sol-gel state diagram

Phase separation, aggregation and gelation are general phenomena of thermal treated protein solutions, and is generally governed by many factors, including pH, protein type, and concentration. The sol-gel state diagram was plotted based on least gelling concentration (LGC) to systematically demonstrate the gelation behavior of SPI, LPI and WPI ascribed to various protein concentrations and pH (Fig. 1). The LGC of SPI, LPI, and WPI showed different pH patterns. At pH 7.0, WPI had a lower LGC of around 8% (*w/w*), indicating its stronger gelling ability compared to pH 3.0 (12%, *w/w*), and 5.0 (10%, *w/w*) and 9.0 (12%, *w/w*). Despite having similar LGC (12%, *w/w*) at pH 3.0 and 9.0, the gel strength of WPI formed at pH 9.0 was much greater than the former, which will be discussed in section 3.1.2 and 3.1.3. This finding was in accordance with the results of SDS-PAGE patterns (Fig. 3e-f) due to the hindered disulfide-mediated polymerization reactions at acidic pH (Monahan, et al., 1995). On the contrary, the LGC of SPI and LPI were the lowest at pH 3.0 (12%, *w/w*) compared to pH 7.0 (14%, *w/w*) and pH 9.0 (14 and 16%, *w/w*), respectively. Moreover, when pH reached its isoelectric point (pI, pH 4-5), where effective net charge of proteins was nearly the lowest, microphase separation occurred for all proteins, resulting in microgel formation. With an increasing protein concentration (e.g. over 10%, *w/w*), WPI was further associated into fractal aggregates and eventually form self-standing gels (often called particulate gels), whereas phase separation was observed between the protein rich and protein poor phases for SPI and LPI. It was consistent with He, et al. (2021) that WPI formed heat-induced particulate gels when pH approached pI as sufficient aggregation resulted in coagulation (Monahan, et al., 1995). The discrepancies among proteins probably due to the superior high solubility of WPI (94.64%) at pH 5.0

compared to LPI (42.39%) and SPI (2.55%) as reported in our previous work (Tang, et al., 2023b), allowing more proteins to participate in gel formation and fewer insoluble proteins adversely affected it. Therefore, it is to worthy note that it is the electrostatic interactions, i.e. net charge of the proteins rather than pH determined the interactions between proteins.

3.1.2. Rheological analysis

The dynamic rheological measurements of SPI, LPI, and WPI gels under different pH conditions were conducted by temperature sweeps to observe their gelation behavior upon heating. Storage modulus (G′), represents energy stored and recovered per oscillation, indicating a material's solid-like elastic characteristics. Loss modulus (G″), refers to the energy dissipated and lost during an oscillation, indicating a material's fluid-like viscous features (Tunick, 2011). The loss tangent (tan δ), defined as the ratio of G″ to G′, reflects a better three-dimensional network at lower values. The G′, G" and tan δ of SPI, LPI, and WPI gels after the cycles of heating and cooling were recorded at 25 °C and shown in Table 1. Overall, all samples showed much higher G′ than G″ (except LPI-9), indicating their preponderantly solid-like properties (tan $\delta < 1$). The gelation behavior of SPI, LPI, and WPI were clearly different depending on pH. For example, SPI showed the same magnitude of G′ at different pH conditions, peaking at pH 9.0, followed by 7.0 and 3.0, and 5.0, while LPI showed a significant decrease over two magnitudes when pH was adjusted from 3.0 to 7.0, 5.0, and 9.0. There was no significant difference in letters of G′ among SPI-3, SPI-5, SPI-7, and SPI-9 gels (Table 1), even if there were noticeable differences observed among them. This might because the G′ values of all protein gels at different pH levels (3.0, 5.0, 7.0, and 9.0) were compared, and among them the G′ values of WPI-7 (26272 ± 846 Pa) and WPI-9 (16115 ± 629 Pa) were two magnitudes higher than those of SPI (from 177 ± 62 to 946 ± 37 Pa), which might result in no significant differences in letters among SPI. Further one-way analysis of variance on SPI (SPI-

3, SPI-5, SPI-7, SPI-9) alone (without WPI and LPI) confirmed the assumption that the G′ of SPI-5 (177 ± 62^{A} Pa) was significantly lower ($p \leq 0.05$) than SPI-3 (568 ± 155^{B} Pa) and SPI-7 (177 ± 62^{BC} Pa), and SPI-9 (946 ± 37^{C} Pa). Significant different ($p \leq 0.05$) among protein gels was denoted by different letters (A, B, C). On the contrary, the gel properties of WPI decreased exponentially when adjusting pH from pH 7.0 (G′ = 26271.90 Pa, tan δ = 0.12) to pH 9.0 (G′ = 16115.00 Pa, tan δ = 0.09), 5.0 (G′ = 7295.00 Pa, tan δ = 0.18) and 3.0 (G′ = 4965.00 Pa, tan δ = 0.11). This was in accordance with the electrophoretic patterns shown in Fig. 3 that the driving force for aggregation and gelation varied from protein to protein. SH/SS reaction (disulphide interaction) dominated the aggregation of β-Lg (primary constituent of WPI), making the gel of WPI stronger than other proteins (Visschers, et al., 2005). However, the reactivity of free sulphydryl groups is directly related to its acidic dissociation constant (pKa), which is around 8.3 when it is fully exposed in water, indicating that thiol/disulfide exchange is inhibited at acidic pH, thus preventing the development of disulphide bound aggregation and impairing its rheological properties (Kornet, et al., 2021; Visschers, et al., 2005). Despite lowering pH reduced sulphydryl reactivity, however, the reduction in electrostatic repulsion promoted protein aggregate growth and thereby promoted the formation of disulphide bonds (Visschers, et al., 2005). Furthermore, the tan δ of WPI-3 (0.11), WPI-7 (0.12), and WPI-9 (0.09) were very low, and no significantly difference ($p > 0.05$) was observed among them, indicating that degree of their solid-like character was practically independent of pH.

It is notable that the highest network strength of LPI was found at pH 3.0 (G′ = 5366.00 Pa, tan δ = 0.10), and showed comparable to WPI-3 (G′ = 4965.00 Pa, tan δ = 0.11), or even significantly higher ($p \leq 0.05$) than SPI-3 (G′ = 568.15 Pa, tan δ = 0.23), which indicating the potential replacement of WPI and SPI by LPI under acidic conditions in gel related food systems. This could attribute to the significantly higher surface hydrophobicity (Ho) of LPI at pH 3.0 compared to that of WPI and SPI, as reported in our previous study (Tang, et al., 2023b),

suggesting that more buried hydrophobic sites exposed resulted in disulfide bridging and hydrophobic aggregation. Additionally, LPI showed fluid-like viscous properties at pH 9.0 due to its similar values of G′ (47.09 Pa) and G″ (47.71 Pa) and subsequent high tan δ (tan δ = 1.01 > 1), which was likely caused by the inhibited protein-protein interactions due to its strong repulsion forces under alkaline conditions (Kim, et al., 2016). There was a comparable lower G′ and G″ of SPI and LPI at pH 5.0 (near pI), indicating that the gel network of SPI-5 and LPI-5 were softer and had less elastic and viscous deformation resistance (Herranz, Piñeiro, Borderías, & Tovar, 2017; Moreno, et al., 2020). This probably due to the reduced electrostatic repulsion and increased hydrophobic interactions promoted random protein aggregation and particulate aggregates formation as pH approached pI (Zhu, Huang, & Chen, 2022). WPI-5, however, displayed significantly higher ($p \leq 0.05$) G′ and G" than SPI-5 and LPI-5. The relatively high solubility of WPI than SPI and LPI at pH 5.0 as reported by our previous findings (Tang, et al., 2023b), might contribute to its higher rheological properties by allowing more proteins to participate in gel formation. However, no significant difference ($p > 0.05$) of tan δ were found in SPI-5 (0.22), LPI-5 (0.18) and WPI-5 (0.18), indicating the noticeable solid-like properties of these samples (tan δ < 1) as well as their similar degree of viscoelasticity.

The rheological properties of protein gels can be affected by structural changes due to the forming and breaking bonds spontaneously or by applied forces between particles over a range of angular frequency between 0.628 and 62.83 rad/s. The logarithms of G′ and frequency of all the samples (except LPI-9) exhibited solid-like elastic behaviour (G′ > G″). Moreover, the G′ values of WPI were significantly higher than that of SPI and LPI under pH 5.0, 7.0 and 9.0, whereas presented similar G′ values with LPI at pH 3.0 at angular frequency between 0.628 and 62.83 rad/s (Fig. 2), which confirmed the temperature sweep results (Table 1). Generally,

gels can be divided into physical gels, entanglement networks, and covalently cross-linked gels (Gunasekaran & Ak, 2000; Tunick, 2011). To further identify the gel structure and its characteristics, power-law model ($\log G' = n' \log \omega + K'$, $\log G'' = n'' \log \omega + K''$) were employed to fit and analyze the relationship between G′, G″ and angular frequency (0.628-62.83 rad/s). Based on equation (1, 2), the fitted parameters (K′, K″, n′, and n″), which describe gel strength and the proximity to a covalent gel (Ge, et al., 2023), respectively, were calculated and summarized in Table 2. Covalently cross-linked gels (strong gels) are characterized by permanent network of covalent bonds with little G′ vs. frequency dependence (ideally $n' = 0$) (Gunasekaran, et al., 2000). Entanglement networks, commonly regarded as soft gels, exhibited strong G′ vs. frequency independence and even a G′-G″ crossover that transitioned from viscous (fluid-like) to elastic (solid-like) behavior as frequency increased (Stading & Hermansson, 1990). Physical gels, which is intermediate between the two, have some frequency independence but no G′-G″ crossover (Tunick, 2011). WPI-7 and WPI-9 showed significantly higher K′ and K″ parameters ($p \leq 0.05$) in comparison to other samples, indicating greater gel rigidity or firmness with more elastic and viscous resistance to deformation, respectively (Table 2) (Moreno, et al., 2020). Moreover, the correlation coefficients, n′ and n″, were found lower and similar in both WPI-7 and WPI-9 (n' and $n'' < 0.1$), which indicated their G′ and G″ were practically independent of time scale, and confirmed the temporal stabilization caused by the covalent bonds in the gel matrix (Herranz, Tovar, Solo-de-Zaldívar, & Borderias, 2012; Moreno, et al., 2020). Additionally, no significantly difference in K′ and K″ between LPI-3 and WPI-3 were observed, but they were significantly higher ($p \leq 0.05$) than SPI-3, suggesting that WPI and SPI might be substituted by LPI in acidic gel related food systems. Similarly, LPI-7 demonstrated significantly higher K′ and K″ ($p \leq 0.05$) compared to SPI-7, implying the possibility of substituting LPI for SPI in neutral food systems.

3.1.3. Mechanical properties

As mechanical characterization is critical in understanding whether a material is suitable for a particular application, the textural properties of thermal-induced SPI, LPI, and WPI gels were characterized as a function of pH (Table 4). Hardness and springiness, which is defined as the maximum force required to compress a food in the first compression cycle ("first bite") and the height of a sample that recovers between the first and second bite, respectively, are very important parameters for gels (Pons & Fiszman, 1996). As shown in Table 4, the mechanical properties of SPI-5, LPI-5, and LPI-9 were not determined since no self-standing gel formed，which prevented them from simulating chewing by compressing a "bite-size" piece. As expected, pH had a significantly effect on the hardness of gels. For instance, the highest hardness was obtained in WPI-7 (1930.95 g) followed by WPI-9 (1202.44 g), which were extremely higher than all other tested samples. This result demonstrated WPI gel formed at neutral and alkaline conditions showed higher firmness due to more covalent cross-linking interactions (especially disulfide bonding) between protein particles (Yang, Ke, & Li, 2021), and were consistent with the results shown in SDS-PAGE (Fig. 3) and rheological parameters (Table 1, 2 and Fig. 2). The discrepancies in gel hardness between these proteins might be due to the compositions of protein subunits and secondary structures in gels as well as the intermolecular interactions for gel network formation. When heated, WPI gels showed a greater hardness that was probably attributed to disulphide bonds (Dissanayake, et al., 2013; Kornet, et al., 2021). Thermal-induced legume gels, however, are generally induced by non-covalent bonds rather than disulphide bonds due to their limited sulfur amino acid content, resulting in relatively low gel hardness (Ge, et al., 2023; Kornet, et al., 2021). Interestingly, LPI-3 (606.48 g) was found to have comparable hardness to WPI-3 (545.95 g) and significantly higher ($p \leq 0.05$) than SPI-3 (125.95 g). Moreover, LPI-7 (461.78 g) also showed significantly stronger hardness ($p \leq 0.05$) than SPI-7 (251.82 g), indicating the relatively higher gel firmness of LPI-

7 than SPI-7. This discriminate could be attributed to the higher solubility of LPI than SPI as reported in our previous work (Tang, et al., 2023b), allowing more proteins to take part in the gel formation process, resulting in more ordered gel networks.

Springiness can be considered to reflect the elasticity properties of gels. Gel springiness did not exhibit appreciable changes for WPI in different pH conditions, where WPI-5 was even slightly lower than WPI-3 and leveled off at higher pH, although their hardness was significantly different. As reported, besides the gel hardness, gel's microstructure had a positive effect on the springiness (Ge, et al., 2023). The springiness of LPI peaked at pH 3.0 and decreased significantly at higher pH ($p \leq 0.05$), whereas SPI achieved the highest springiness at pH 9.0, and decreased at lower pH ($p \leq 0.05$). More specifically, LPI-3 exhibited a similar or superior springiness to WPI-3 and SPI-3, and LPI-7 demonstrated higher springiness to SPI-7, indicating the better shape recovery of LPI-3 and LPI-7 gels. Based on the overall mechanical analysis, LPI might be served as a good alternative to WPI in terms of thermal-induced gel systems at acidic conditions, and to SPI in acidic and neutral conditions.

3.1.4. Gel water retention

WHC of a gel refers to its ability to prevent water leaking out from its three-dimensional structure. As shown in Table 4, the WHC of WPI at pH away pI reached the maximum values (over 90%), demonstrating that almost all water can be retained in the gel due to the fine-stranded gels (nm) formed. Although WPI-5 had higher G′ and hardness compared to WPI-3, the WHC of the former was lower. This probably due to the relative higher tan δ of WPI-5 (0.18) than WPI-3 (0.11), which demonstrated that WPI-5 had less solid-like character (less ideal-network fraction) and therefore less WHC. The WHC of SPI was found highest in pH 9.0, compared with neutral and acidic pH, however, highest WHC for LPI was noticed at pH 3.0, followed by pH 7.0. These phenomena were in agreement with the rheological (Fig. 2 and Table 1, 2) and textural results (Table 4), which might related to the enhanced formation of

proteins-protein aggregates due to more exposure of hydrophobic residues of LPI at acidic pH, leading to a better gel network and higher WHC (Hu, et al., 2013).

3.2. Physicochemical and structural fingerprinting

3.2.1. Gel electrophoresis

The molecular weight distribution of thermal-induced soy, lentil and whey protein gels prepared at different pH levels are shown in Fig. 3a-f. The samples were subjected to unreducing (SDS) and reducing conditions (SDS + DTT) to disrupt non-covalent bonds and both non-covalent bonds and S-S bonds within proteins that were either formed during heating or naturally present, respectively (Djoullah, Djemaoune, Husson, & Saurel, 2015).

The major protein components of SPI are 11S (glycinin, 320-360 kDa) globulins and 7S (β-conglycinin, 150-200 kDa) globulins. Five major subunits: A1aB2 (G1, 58 kDa), A1bB1b (G2, 58 kDa), A2B1a (G3, 58 kDa), A3B4 (G4, 62 kDa), and A5A4B3 (G5, 69 kDa) were identified as constituting 11S (glycinin) globulins (hexameric structure), with each subunits (58-69 kDa) consisting of an acidic (～35 kDa) and a basic (～20 kDa) polypeptides linked by a disulfide bond (Adachi, et al., 2003; Nielsen, 1985). 7S (β-conglycinin) globulins have a trimeric structure made up of three prevalent subunits: α (～ 67 kDa), α′ (～ 71 kDa) and β (～ 50 kDa) linked together by noncovalent bonds (Maruyama, et al., 1998; Wang, et al., 2022).

As shown in Fig. 3a, thermal-treated SPI samples showed high-molecular weight aggregates (> 180 kDa) with dramatically diminished glycinin (11S) acidic, basic subunits under non-reducing SDS-PAGE conditions. The aggregate bands, however, mostly vanished under reducing conditions and the bands representing the basic and acidic subunits of glycinin were mostly restored (Fig. 3b). Therefore, the formation of high-molecular weight aggregates during thermal gelation process was demonstrated among sulfhydryl-containing polypeptides (e.g.

11S acidic and basic subunits) cross-linked by disulphide bonds (Tanger, et al., 2022; Wang, et al., 2022). Similar findings were reported by Wang, et al. (2022) after heat treatment of SPI solutions by both conventional heating and moderate electric field heating at 85 ℃ for 30 min.

All typically expected individual protein fractions (11S and 7 S subunits) appeared in thermal-induced LPI gels regardless of pH treatment conditions (Fig. 3c-d). Similar phenomena were observed for thermal-induced LPI protein gels. The fraction ascribed to 11S acidic (～40 kDa) and basic subunits (～20 kDa) decreased but more high molecular aggregates (> 180 kDa) accumulated under non-reducing conditions compared to the corresponding reducing conditions (Fig. 3c-d). Similar molecular weight profiles were observed when comparing the same protein sample (SPI and PPI) regardless of pH treatment. It was also reported by Ge, et al. (2023) that heat-induced plant protein gels prepared at pH 3.0 or pH 7.0 did not show significant differences in SDS patterns. The electrophoretic patterns of heated SPI and LPI samples under NR conditions showed many bands left regardless of pH, suggesting that disulfide bonds may not be the major forces responsible for gel formation in these proteins (Fig. 3a, c). This result agreed with previous studies that heat-induced gel formation of plant proteins was mainly caused by hydrophobic interactions rather than disulfide bonds due to their low cysteine content (Sun & Arntfield, 2012; Tanger, et al., 2022).

The polymerization of WPI, however, is profoundly influenced by pH. β-Lactoglobulin (β-Lg, ～18 kDa) and α-Lactalbumin (α-La, ～14 kDa) are the most abundant fractions in WPI. These subunits diminished at pH 3.0 and vanished at higher pH conditions under non-reducing conditions (Fig. 3e), while showing increased intensity under reducing conditions (Fig. 3f). Similar results were reported by Shimada and Cheftel (1989) that the intensity of these protein fractions decreased slightly at pH 2.5 compared to that at pH 7.5. It may be ascribed to the diminished alternation between thiolate and thiol and the thiol/disulfide, preventing the cross-

linking of β-lactoglobulin at acidic conditions (Monahan, et al., 1995). Disulfide-mediated polymerization reactions, however, were favored at relative higher pH, resulting in more high molecular protein aggregates (Monahan, et al., 1995). These results could explain the highest gelation performance of WPI at pH 7.0 as shown in section 3.1 since the SH/S-S interchange reactions contribute majorly to the gel network formation and good gel elasticity near neutral conditions (Shimada, et al., 1989).

3.2.2. Fourier transform infrared (FTIR) spectral profiling

Since the amide I region (1700-1600 cm^{-1}) is associated primarily with the stretching vibration of C=O bonds and very sensitive to change during gelation process, ATR-FTIR was performed to observe the structural and conformation changes of SPI, PPI and WPI gels as a function of pH (Zhou, Tobin, Drusch, & Hogan, 2021). The deconvoluted FTIR spectra and relative area percentages of different secondary structures for these gel samples are shown in Fig. 4 and Table 4. The secondary structure of these protein samples were dominated by β-sheet structure (intra/intermolecular), which was in accordance with the findings of Zheng, et al. (2021), as shown by the most prevalent secondary structure in SPI, PPI, and WPI, accounting for 34.30-43.67%, 36.55-41.71%, and 36.42-44.93%, respectively. The absorption intensities for SPI gels attributable to α-helix (from 21.73 to 26.55 and 31.00%), intramolecular β-sheet (from 19.15 to 20.55 and 24.24%), and intermolecular/aggregated β-sheet (from 15.15 to 18.95 and 19.42%) increased as shifting the pH from 3.0 to 7.0 and further to 9.0, whereas the absorption intensities of β-turn (from 11.09 to 8.43 and 7.94%), random coil (from 32.78 to 25.46 and 17.33%) deceased. This result was in accordance with the enhanced gelation properties for SPI at pH 9.0 since alkaline treatment can partly unfold SPI by disrupting hydrogen bonding, exposing buried free SH and active side chains, and facilitating protein aggregation in conjunction with heating (Jo & Chen, 2023; Zhang, Huang, Roopesh, & Chen, 2022). Furthermore, α-helix and intramolecular/aggregated β-sheet was reported to possess larger

surface area, providing greater opportunities for intermolecular hydrogen bonding, protein-protein hydrophobic interactions and covalent bonding, resulting in the formation of more densely cross-linked protein gel network (Moreno, et al., 2020; Zheng, et al., 2021).

Contrarily, a different trend was observed for WPI that the highest content of α-helix and intermolecular (aggregated) β-sheet were found in WPI-7 (29.20% and 22.07%), which were higher than WPI-9 (25.00% and 19.45%), WPI-5 (18.93% and 18.47%) and WPI-3 (16.78% and 12.05%), respectively. The activation energy of β-Lg denaturation decreases as the pH increases, while no apparent trend for α-La (Oldfield, Singh, Taylor, & Pearce, 2000). With an increase in pH, the repulsion of ionized groups may facilitate protein unfolding (denaturation) by requiring less energy (lower activation energy). Moreover, the pKa of sulphydryl groups is approximately 8.3, and its reactivity is directly related to pKa (Visschers, et al., 2005). Therefore, at acidic pH, thiol/disulfide exchange was inhibited, which prevented disulphide bound aggregations from forming, and thus adversely affected its gel performance. Intermolecular interactions (aggregation) can, however, be hindered by the protein charge repulsion since it can reduce the number of favorable collisions that would lead to aggregation between denatured β-Lg (Oldfield, et al., 2000). The formation of disulfide bonds might be affected by steric effects while whey proteins were heated (Chandrapala, 2008). This might explain the lower rheological and textural properties of WPI-9 compared to WPI-7. Moreover, the relative higher percentage of intermolecular (aggregated) β-sheet in WPI-7 (22.07%) than WPI-9 (19.45%) might help support this explanation (Table 4).

There were no significantly difference ($p > 0.05$) between LPI-3 and WPI-3 in regarding to the deconvoluted relative area percentage (Table 4) of α-helix (19.83 and 16.78%), intramolecular β-sheet (22.08 and 24.37%), intermolecular/aggregated β-sheet (14.47 and 12.05%), β-turn (9.36 and 8.16%), and side chain (0.05 and 0.04%), which might explain their similar rheological and textural properties as clearly discussed previously. Moreover, LPI-3 processed

greater levels of intramolecular β-sheet since acidic treatment enhanced its surface hydrophobicity as reported by our previous work (Tang, et al., 2023b), and might be responsible for its higher thermal gelation properties than other pH conditions.

3.2.3. Appearance and colour

To determine the quality of gels, appearance and colour are also important indicators. The appearance and colour values of thermal-induced SPI, LPI, and WPI gels as a function of pH (3.0, 5.0, 7.0, and 9.0) are shown in Fig. 5a-b. The visual appearance and colour values of these gels were highly sensitive to pH, and different protein had different response to pH alteration. According to Fig. 5a, SPI can form self-standing gels as observed visually except pH 5.0, and gels became stiffer and relatively transparent at higher pH values. In contrast, LPI formed self-standing gels at pH 3.0 and 7.0, whereas no gel formed at pH 9.0, which was in consistence with previous analysis. WPI can form self-supporting gels regardless of test pH under thermal treatment, with the gels varying from white, opaque to translucent in appearance as pH shifted away from 5.0. This phenomena agreed with He, et al. (2021); Wang, et al. (2020) and probably because WPI formed disordered particulate gels that scatter more light and increased the turbidity of gels when electrostatic repulsion was limited (pH near pI), while fine-stranded gels formed when repulsive forces dominated (pH away from pI) (Langton, et al., 1992).

As shown in Fig. 5b, the highest $L*$ and *WI* were found for all thermal protein gels at pH 5.0 (near pI). The $L*$ and *WI* of all gels decreased as pH shifted far away from pI, which was in accordance with their more translucent and brownish-black appearance (Fig. 5a). Among them, WPI generally represented higher $L*$ and *WI* (except WPI-3), while LPI showed the highest $a*$ and $b*$ values, demonstrating the creamy-white of WPI and redness colour properties of LPI gels, respectively. Therefore, the variations in colour properties of gel were affected by various factors, such as the original colour of protein sources and gelation conditions. Besides,

decolorization could be performed to improve the application of LPI to certain foods for colour concern (Tang, et al., 2023b).

3.2.4. Microstructural analysis

CLSM was carried out to investigate the microstructure of the SPI, LPI, and WPI gels at the micrometer length scale and demonstrated in Fig. 6. The proteins stained with rhodamine B appeared as red and depicted as red areas, whereas the black area showed the voids or pores in between the protein particles. It is notable that the microstructure of globular proteins depends on the strength of the electrostatic repulsions. For example, at pH 5.0 (near pI), all protein formed microgels with large protein particles (10-50 μm), heterogeneous and irregular shapes. At pH 3.0, SPI formed a heterogeneous gel structure with larger clusters (～100 μm) at microscale. As pH further shifted to neutral and alkaline conditions, the microstructure changed from a larger roundish structure surrounded by irregular small scale aggregates to a more homogeneous structure with much smaller aggregates (～10 μm). Similar results were reported that as electrostatic repulsion was reduced, more heterogeneous microstructures were observed for SPI. Additionally, repulsive interactions were reported to facilitate the formation of chains, leading to the development of interconnected strands, attractive interactions, however, promote the formation of coarser network (Nicolai, 2019).

In contrast, thermal-induced LPI and WPI samples regardless of pH (except 5.0) showed homogeneous and fine gel networks since the diameter of the gel-forming protein aggregates were within nanoscale and could not be observed by CLSM. Similar results have been reported by Langton, et al. (1992) that the microstructure gels of whey protein, particularly β-lactoglobulin, converted from white particulate at pH 4-6 (pI) to transparent fine-stranded at pH > 6 or pH < 4. These discrepancies in gelation properties can be attributed to differences in

protein composition and structure properties as well as intermolecular interactions that cause gelation to occur (Ge, et al., 2023).

3.3. Hierarchical cluster analysis

Hierarchical cluster analysis (HCA) is a clustering method that can be used to distinguish the similarity of thermal-induced SPI, LPI and WPI gels obtained under different pH conditions (Fig. 7). Colour differences were determined by clustering the columns of these samples and normalizing the raw data into Z-scores. It was clear that three major groups were clustered. Group 1 and group 3 contained SPI-3 and WPI-7, showing the weakest and highest gel performance, respectively. Group 2 consisted of seven samples with three subclusters: the first (LPI-3, WPI-3, and WPI-9), the second (WPI-5), and the third (SPI-7, SPI-9, and LPI-7). Consequently, the HCA analysis demonstrated a similarity between LPI and WPI gels at pH 3.0, which further confirmed the potential applications of substituting WPI with LPI in acidic gel-related food products. Moreover, the superior gel performance of LPI over SPI at acidic and neutral condition further showcases the potential utilization of LPI as a substitute for SPI in related food products.

4. Conclusions

The present study investigated the influence of pH (3.0, 5.0, 7.0, and 9.0) on the structural, rheological, and mechanical properties of SPI, LPI, and WPI gels. This study demonstrated that proteins from different sources had different response to pH regarding to their gelation performance. Gel electrophoresis revealed that during the thermal gelation process, only specific subunits, like 11S acidic and basic subunits in plant proteins (SPI and LPI) were involved in disulfide bonds formation. Notably, partial β-Lg and α-La participated in the formation of disulfide bonds under pH 3.0, whereas nearly all fractions in WPI were involved under higher pH conditions. The elevation of pH resulted in the increasing content of the α-

helix, intramolecular β-sheet, and intermolecular/aggregated β-sheet may contribute to the enhanced gel performance of SPI-9, while the highest content of α-helix and intermolecular (aggregated) β-sheet was observed in WPI-7, followed by WPI-9. At pH 3.0, LPI and WPI exhibited similar secondary structures with relative higher levels of intramolecular β-sheet, as well as comparable rheological properties (5366.00 and 4965.00 Pa of G′), and mechanical properties (606.48 and 545.95 g of gel hardness), homogenous and compact microstructural properties. As pH increased from 3.0 to 7.0 and 9.0, SPI presented enhanced gel performance, as evidenced by an increase in G′ from 568.15 to 691.60 and 946.05 Pa. Conversely, LPI showed decreased gel properties, with G′ decreasing from 5366.00 to 2026.00 and 47.09 Pa. The highest gel performance of WPI was observed at pH 7.0, with G′ increasing from 4965.00 to 26271.90 Pa, followed by a decline to 16115.00 Pa as pH shifted from 3.0 to 7.0 and 9.0. Moreover, HCA analysis coupled with rheological and textural analysis confirmed the potential of LPI as a substitute for WPI in gel-related food systems under acidic environments, but also for SPI in acidic and neutral ones. Understanding the thermal gelation performance of protein from different sources at different pH conditions is therefore beneficial for LPI in gel-based products formulation. Further studies can be conducted to investigate how heating regulates the gelling mechanism and performance of LPI in practical food systems, such as dairy and meat-based analogues.

Credit author statement

Qi Tang: Investigation, Conceptualization, Data curation, Methodology, Writing - original draft, Writing - review & editing. **Yrjö H. Roos:** Supervision, Writing - review & editing. **Song Miao:** Project administration, Conceptualization, Supervision, Funding acquisition, Writing - review & editing.

Declaration of competing interest

The authors declare that they have no known competing financial interests or personal relationships that could have appeared to influence the work reported in this paper.

Acknowledgement

The authors acknowledge the financial support from the China Scholarship Council (No. 201908320414) and Horizon 2020 European Union funded research innovation programme SMART PROTEIN Project (No: 862957), which have enabled us to carry out this study.

References

Adachi, M., Kanamori, J., Masuda, T., Yagasaki, K., Kitamura, K., Mikami, B., & Utsumi, S. (2003). Crystal structure of soybean 11S globulin: glycinin A3B4 homohexamer. *Proceedings of the National Academy of Sciences, 100*(12), 7395-7400. http://doi.org/10.1073/pnas.0832158100.

Chandrapala, J. J. S. (2008). *Effect of concentration, pH and added chelating agents on the colloidal properties of heated reconstituted skim milk.* Monash University.

Daniloski, D., McCarthy, N. A., Auldist, M. J., & Vasiljevic, T. (2022). Properties of sodium caseinate as affected by the β-casein phenotypes. *Journal of Colloid and Interface Science, 626*, 939-950. http://doi.org/10.1016/j.jcis.2022.07.021.

Dissanayake, M., Ramchandran, L., Piyadasa, C., & Vasiljevic, T. (2013). Influence of heat and pH on structure and conformation of whey proteins. *International Dairy Journal, 28*(2), 56-61. http://doi.org/10.1016/j.idairyj.2012.08.014

Djoullah, A., Djemaoune, Y., Husson, F., & Saurel, R. (2015). Native-state pea albumin and globulin behavior upon transglutaminase treatment. *Process Biochemistry, 50*(8), 1284-1292. http://doi.org/10.1016/j.procbio.2015.04.021.

Ge, J., Sun, C., Chang, Y., Li, S., Zhang, Y., & Fang, Y. (2023). Understanding the differences in heat-induced gel properties of twelve legume proteins: A comparative study. *Food Research International, 163*, 112134. http://doi.org/10.1016/j.foodres.2022.112134.

Gunasekaran, S., & Ak, M. M. (2000). Dynamic oscillatory shear testing of foods—selected applications. *Trends in Food Science & Technology, 11*(3), 115-127. http://doi.org/10.1016/S0924-2244(00)00058-3.

He, Z., Ma, T., Zhang, W., Su, E., Cao, F., Huang, M., & Wang, Y. (2021). Heat-induced gel formation by whey protein isolate-Lycium barbarum polysaccharides at varying pHs. *Food Hydrocolloids, 115*, 106607. http://doi.org/10.1016/j.foodhyd.2021.106607.

Herranz, B., Piñeiro, L., Borderías, A. J., & Tovar, C. A. (2017). Effect of long-term frozen storage on the rheological properties of pressurized glucomannan gels. *Food Hydrocolloids, 67*, 224-228. http://doi.org/10.1016/j.foodhyd.2016.11.021.

Herranz, B., Tovar, C. A., Solo-de-Zaldívar, B., & Borderias, A. J. (2012). Effect of alkalis on konjac glucomannan gels for use as potential gelling agents in restructured seafood products. *Food Hydrocolloids, 27*(1), 145-153. http://doi.org/10.1016/j.foodhyd.2011.08.003.

Hu, H., Fan, X., Zhou, Z., Xu, X., Fan, G., Wang, L., Huang, X., Pan, S., & Zhu, L. (2013). Acid-induced gelation behavior of soybean protein isolate with high intensity ultrasonic pre-treatments. *Ultrason Sonochem, 20*(1), 187-195. http://doi.org/10.1016/j.ultsonch.2012.07.011.

Jo, Y.-J., & Chen, L. (2023). Gelation behavior of lentil protein aggregates induced by sequential combination of glucono-δ-lactone and transglutaminase. *Food Structure, 36*, 100312. http://doi.org/10.1016/j.foostr.2023.100312.

Kim, J. H. J., Varankovich, N. V., & Nickerson, M. T. (2016). The effect of pH on the gelling behaviour of canola and soy protein isolates. *Food Research International, 81*, 31-38. http://doi.org/10.1016/j.foodres.2015.12.029.

Kornet, R., Shek, C., Venema, P., van der Goot, A. J., Meinders, M., & van der Linden, E. (2021). Substitution of whey protein by pea protein is facilitated by specific fractionation routes. *Food Hydrocolloids, 117*, 106691. http://doi.org/10.1016/j.foodhyd.2021.106691.

Kurpiewska, K., Biela, A., Loch, J. I., Lipowska, J., Siuda, M., & Lewiński, K. (2019). Towards understanding the effect of high pressure on food protein allergenicity: β-lactoglobulin structural studies. *Food Chemistry, 270*, 315-321. http://doi.org/10.1016/j.foodchem.2018.07.104.

Lakemond, C. M., de Jongh, H. H., Hessing, M., Gruppen, H., & Voragen, A. G. (2000). Soy glycinin: influence of pH and ionic strength on solubility and molecular structure at ambient temperatures. *Journal of Agricultural and Food Chemistry, 48*(6), 1985-1990. http://doi.org/10.1021/jf9908695.

Langton, M., & Hermansson, A.-M. (1992). Fine-stranded and particulate gels of β-lactoglobulin and whey protein at varying pH. *Food Hydrocolloids, 5*(6), 523-539. http://doi.org/10.1016/S0268-005X(09)80122-7.

Li, Q., & Zhao, Z. (2018). Interaction between lactoferrin and whey proteins and its influence on the heat-induced gelation of whey proteins. *Food Chemistry, 252*, 92-98. http://doi.org/10.1016/j.foodchem.2018.01.114.

Markoska, T., Daniloski, D., Vasiljevic, T., & Huppertz, T. (2021). Structural changes of β-casein induced by temperature and pH analysed by nuclear magnetic resonance, Fourier-transform infrared spectroscopy, and chemometrics. *Molecules, 26*(24), 7650. http://doi.org/10.3390/molecules26247650.

Maruyama, N., Katsube, T., Wada, Y., Oh, M. H., Barba De La Rosa, A. P., Okuda, E., Nakagawa, S., & Utsumi, S. (1998). The roles of the N-linked glycans and extension regions of soybean β-conglycinin in folding, assembly and structural features. *European journal of biochemistry, 258*(2), 854-862. http://doi.org/10.1046/j.1432-1327.1998.2580854.x.

Mckenzie, H. A., & Sawyer, W. H. (1967). Effect of pH on β-lactoglobulins. *Nature, 214*, 1101-1104. http://doi.org/10.1038/2141101a0.

Monahan, F. J., German, J. B., & Kinsella, J. E. (1995). Effect of pH and temperature on protein unfolding and thiol/disulfide interchange reactions during heat-induced gelation of whey proteins. *Journal of Agricultural and Food Chemistry, 43*(1), 46-52. http://doi.org/10.1021/jf00049a010.

Moreno, H. M., Domínguez-Timón, F., Díaz, M. T., Pedrosa, M. M., Borderías, A. J., & Tovar, C. A. (2020). Evaluation of gels made with different commercial pea protein isolate: Rheological, structural and functional properties. *Food Hydrocolloids, 99*, 105375. http://doi.org/10.1016/j.foodhyd.2019.105375.

Ng, S. W., Lu, P., Rulikowska, A., Boehm, D., O'Neill, G., & Bourke, P. (2021). The effect of atmospheric cold plasma treatment on the antigenic properties of bovine milk casein and whey proteins. *Food Chemistry, 342*, 128283. http://doi.org/10.1016/j.foodchem.2020.128283.

Nicolai, T. (2019). Gelation of Food Protein-Protein Mixtures. *Advances in colloid and interface science, 270*, 147-164. http://doi.org/10.1016/j.cis.2019.06.006.

Nicolai, T., & Chassenieux, C. (2019). Heat-induced gelation of plant globulins. *Current Opinion in Food Science, 27*, 18-22. http://doi.org/10.1016/j.cofs.2019.04.005.

Nielsen, N. C. (1985). The structure and complexity of the 11S polypeptides in soybeans. *Journal of the American Oil Chemists' Society, 62*(12), 1680-1686. http://doi.org/10.1007/BF02541665.

Oldfield, D. J., Singh, H., Taylor, M. W., & Pearce, K. N. (2000). Heat-induced interactions of β-lactoglobulin and α-lactalbumin with the casein micelle in pH-adjusted skim milk. *International Dairy Journal, 10*(8), 509-518. http://doi.org/10.1016/S0958-6946(00)00087-X.

Pereira, R., Bennett, R., Hemar, Y., & Campanella, O. (2001). Rheological and microstructural characteristics of model processed cheese analogues. *Journal of Texture Studies, 32*(5-6), 349-373. http://doi.org/10.1111/j.1745-4603.2001.tb01242.x.

Pons, M., & Fiszman, S. (1996). Instrumental texture profile analysis with particular reference to gelled systems. *Journal of Texture Studies, 27*(6), 597-624. http://doi.org/10.1111/j.1745-4603.1996.tb00996.x.

Puppo, M. C., & Anon, M. C. (1998). Structural properties of heat-induced soy protein gels as affected by ionic strength and pH. *Journal of Agricultural and Food Chemistry, 46*(9), 3583-3589. http://doi.org/10.1021/jf980006w.

Renkema, J. M., Lakemond, C. M., de Jongh, H. H., Gruppen, H., & van Vliet, T. (2000). The effect of pH on heat denaturation and gel forming properties of soy proteins. *J Biotechnol, 79*(3), 223-230. http://doi.org/10.1016/s0168-1656(00)00239-x.

Samaranayaka, A. (2017). Lentil: Revival of poor man's meat. In *Sustainable protein sources* (pp. 185-196): Elsevier. http://doi.org/10.1016/B978-0-12-802778-3.00011-1.

Santana, P., Huda, N., & Yang, T. A. (2015). Physicochemical properties and sensory characteristics of sausage formulated with surimi powder. *Journal of Food Science and Technology, 52*(3), 1507-1515. http://doi.org/10.1007/s13197-013-1145-1.

Shimada, K., & Cheftel, J. C. (1989). Sulfhydryl group/disulfide bond interchange reactions during heat-induced gelation of whey protein isolate. *Journal of Agricultural and Food Chemistry, 37*(1), 161-168. http://doi.org/10.1021/jf00085a038.

Sittikijyothin, W., Sampaio, P., & Gonçalves, M. P. (2007). Heat-induced gelation of β-lactoglobulin at varying pH: Effect of tara gum on the rheological and structural properties of the gels. *Food Hydrocolloids, 21*(7), 1046-1055. http://doi.org/10.1016/j.foodhyd.2006.07.019.

Stading, M., & Hermansson, A.-M. (1990). Viscoelastic behaviour of β-lactoglobulin gel structures. *Food Hydrocolloids, 4*(2), 121-135. http://doi.org/10.1016/S0268-005X(09)80013-1.

Sun, X. D., & Arntfield, S. D. (2012). Molecular forces involved in heat-induced pea protein gelation: Effects of various reagents on the rheological properties of salt-extracted pea protein gels. *Food Hydrocolloids, 28*(2), 325-332. http://doi.org/10.1016/j.foodhyd.2011.12.014.

Tang, Q., Roos, Y. H., & Miao, S. (2023a). Effect of microbial transglutaminase on functional, rheological, and structural properties of lentil protein-casein binary gels. *Food Hydrocolloids, 143*, 108838. http://doi.org/https://doi.org/10.1016/j.foodhyd.2023.108838.

Tang, Q., Roos, Y. H., & Miao, S. (2023b). Plant protein versus dairy proteins: a pH-dependency investigation on their structure and functional properties. *Foods, 12*(2), 368. http://doi.org/10.3390/foods12020368.

Tanger, C., Müller, M., Andlinger, D., & Kulozik, U. (2022). Influence of pH and ionic strength on the thermal gelation behaviour of pea protein. *Food Hydrocolloids, 123*, 106903. http://doi.org/10.1016/j.foodhyd.2021.106903.

Tunick, M. H. (2011). Small-strain dynamic rheology of food protein networks. *Journal of Agricultural and Food Chemistry, 59*(5), 1481-1486. http://doi.org/10.1021/jf1016237.

Vallath, A., Shanmugam, A., & Rawson, A. (2022). Prospects of future pulse milk variants from other healthier pulses-As an alternative to soy milk. *Trends in Food Science & Technology, 124*, 51-62. http://doi.org/10.1016/j.tifs.2022.03.028.

Visschers, R. W., & de Jongh, H. H. (2005). Disulphide bond formation in food protein aggregation and gelation. *Biotechnology advances, 23*(1), 75-80. http://doi.org/10.1016/j.biotechadv.2004.09.005.

Wang, H., Wang, N., Chen, X., Wu, Z., Zhong, W., Yu, D., & Zhang, H. (2022). Effects of moderate electric field on the structural properties and aggregation characteristics of soybean protein isolate. *Food Hydrocolloids, 133*, 107911. http://doi.org/10.1016/j.foodhyd.2022.107911.

Wang, Y., Zhao, J., Zhang, W., Liu, C., Jauregi, P., & Huang, M. (2020). Modification of heat-induced whey protein gels by basic amino acids. *Food Hydrocolloids, 100*, 105397. http://doi.org/10.1016/j.foodhyd.2019.105397.

Yang, X., Ke, C., & Li, L. (2021). Physicochemical, rheological and digestive characteristics of soy protein isolate gel induced by lactic acid bacteria. *Journal of Food Engineering, 292*, 110243. http://doi.org/10.1016/j.jfoodeng.2020.110243.

Zhang, S., Huang, W., Roopesh, M., & Chen, L. (2022). Pre-treatment by combining atmospheric cold plasma and pH-shifting to prepare pea protein concentrate powders with improved gelling properties. *Food Research International, 154*, 111028. http://doi.org/10.1016/j.foodres.2022.111028.

Zheng, L., Regenstein, J. M., Zhou, L., & Wang, Z. (2022). Soy protein isolates: A review of their composition, aggregation, and gelation. *Comprehensive Reviews in Food Science and Food Safety, 21*(2), 1940-1957. http://doi.org/10.1111/1541-4337.12925.

Zheng, L., Wang, Z., Kong, Y., Ma, Z., Wu, C., Regenstein, J. M., Teng, F., & Li, Y. (2021). Different commercial soy protein isolates and the characteristics of Chiba tofu. *Food Hydrocolloids, 110*, 106115. http://doi.org/10.1016/j.foodhyd.2020.106115.

Zhou, B., Tobin, J. T., Drusch, S., & Hogan, S. A. (2021). Dynamic adsorption and interfacial rheology of whey protein isolate at oil-water interfaces: Effects of protein concentration, pH and heat treatment. *Food Hydrocolloids, 116*, 106640. http://doi.org/10.1016/j.foodhyd.2021.106640.

Zhu, P., Huang, W., & Chen, L. (2022). Develop and characterize thermally reversible transparent gels from pea protein isolate and study the gel formation mechanisms. *Food Hydrocolloids, 125*, 107373. http://doi.org/10.1016/j.foodhyd.2021.107373.

Table 1. Rheological parameters (temperature sweep) of heat-induced SPI, LPI and WPI gels as a function of pH.

Samples	Temperature sweep		
	G′ (Pa)	G″ (Pa)	Tan δ
SPI-3	568 ± 155^{a}	130 ± 34^{ab}	0.23 ± 0.00^{e}
LPI-3	5366 ± 110^{c}	558 ± 37^{b}	0.10 ± 0.00^{a}
WPI-3	4965 ± 255^{c}	559 ± 33^{b}	0.11 ± 0.00^{a}
SPI-5	177 ± 62^{a}	36 ± 2^{a}	0.22 ± 0.07^{de}
LPI-5	313 ± 112^{a}	54 ± 7^{a}	0.18 ± 0.04^{cde}
WPI-5	7295 ± 502^{d}	1296 ± 136^{c}	0.18 ± 0.01^{bcd}
SPI-7	692 ± 128^{a}	87 ± 13^{a}	0.13 ± 0.00^{ab}
LPI-7	2026 ± 484^{b}	294 ± 88^{ab}	0.14 ± 0.01^{abc}
WPI-7	26272 ± 846^{f}	3086 ± 631^{d}	0.12 ± 0.02^{a}
SPI-9	946 ± 37^{a}	117 ± 4^{ab}	0.12 ± 0.00^{a}
LPI-9	47 ± 15^{a}	48 ± 15^{a}	1.01 ± 0.01^{f}
WPI-9	16115 ± 629^{e}	1458 ± 57^{c}	0.09 ± 0.00^{a}

Names of samples with numbers indicate the protein isolate gels obtained at the corresponding pH conditions. Significant different ($p \leq 0.05$) among protein gels was denoted by different letters.

770 **Table 2.** Power-law parameters (frequency sweep) of heat-induced SPI, LPI and WPI gels as

771 a function of pH.

Samples	K′ (Pa· s^n)	n′	R^2 Eq. (1)	K″ (Pa· s^n)	n″	R^2 Eq. (2)
SPI-3	480 ± 137^{a}	0.060 ± 0.004^{a}	0.9347	92 ± 36^{a}	0.132 ± 0.004^{de}	0.9741
LPI-3	4942 ± 140^{c}	0.058 ± 0.001^{a}	0.9959	492 ± 77^{c}	0.086 ± 0.020^{abc}	0.9370
WPI-3	4485 ± 173^{c}	0.068 ± 0.001^{ab}	0.9948	498 ± 40^{c}	0.083 ± 0.010^{ab}	0.9838
SPI-5	150 ± 59^{a}	0.094 ± 0.030^{c}	0.9821	28 ± 3^{a}	0.153 ± 0.024^{e}	0.9968
LPI-5	236 ± 44^{a}	0.070 ± 0.003^{ab}	0.9639	45 ± 9^{a}	0.130 ± 0.003^{de}	0.9683
WPI-5	6362 ± 480^{d}	0.095 ± 0.002^{c}	0.9954	1040 ± 83^{d}	0.108 ± 0.012^{bcd}	0.9411
SPI-7	617 ± 120^{a}	0.076 ± 0.000^{abc}	0.9834	77 ± 16^{a}	0.094 ± 0.012^{abc}	0.9240
LPI-7	1773 ± 438^{b}	0.086 ± 0.007^{bc}	0.9985	241 ± 82^{b}	0.112 ± 0.006^{cd}	0.9860
WPI-7	24128 ± 882^{f}	0.062 ± 0.001^{a}	0.9981	2434 ± 89^{f}	0.070 ± 0.004^{a}	0.9267
SPI-9	841 ± 34^{a}	0.070 ± 0.002^{ab}	0.9929	100 ± 5^{a}	0.094 ± 0.010^{abc}	0.9676
LPI-9	65 ± 10^{a}	0.177 ± 0.013^{d}	0.9962	69 ± 4^{a}	0.123 ± 0.007^{d}	0.9946
WPI-9	14821 ± 91^{e}	0.058 ± 0.002^{a}	0.9855	1340 ± 8^{e}	0.076 ± 0.002^{a}	0.9888

772 Names of samples with numbers indicate the protein isolate gels obtained at the corresponding
773 pH conditions. Significant different ($p \leq 0.05$) among protein gels was denoted by different
774 letters.

775

776 **Table 3.** Mechanical properties and water holding capacity (WHC) of thermal-induced SPI,

777 LPI, and WPI gels as a function of pH.

Samples	Hardness (g)	Springiness (%)	WHC (%)
SPI-3	125.95 ± 30.08^{a}	62.66 ± 1.64^{a}	64.96 ± 4.04^{a}
LPI-3	606.48 ± 2.16^{d}	90.66 ± 1.44^{e}	91.17 ± 0.47^{ef}
WPI-3	545.95 ± 14.46^{d}	93.79 ± 3.38^{ef}	92.84 ± 0.40^{fg}
WPI-5	622.05 ± 30.14^{d}	92.69 ± 0.62^{ef}	87.71 ± 2.55^{e}
SPI-7	251.82 ± 55.27^{ab}	70.33 ± 1.70^{b}	73.04 ± 0.68^{b}
LPI-7	461.78 ± 4.89^{cd}	83.66 ± 1.13^{d}	82.99 ± 0.81^{d}
WPI-7	1930.95 ± 79.33^{f}	96.89 ± 2.71^{f}	98.73 ± 0.45^{h}
SPI-9	319.56 ± 14.24^{bc}	76.55 ± 1.77^{c}	77.12 ± 1.33^{c}
WPI-9	1202.44 ± 205.84^{e}	94.14 ± 1.44^{ef}	96.27 ± 0.96^{gh}

778 Names of samples with numbers indicate the protein isolate gels obtained at the corresponding
779 pH conditions. Significant different ($p \leq 0.05$) among protein gels was denoted by different
780 letters.

781

782

783

784

785

786

787

788

789

790

791

792

Table 4. FTIR analysis of thermal-induced SPI, LPI, and WPI gels as a function of pH.

Samples	α-helix	Intramolecular β-sheet	Aggregated β-sheet	β-turn	Random coil	Side chain
SPI-3	21.73 ± 1.00^{bcd}	19.15 ± 0.25^{ab}	15.15 ± 0.87^{b}	11.09 ± 1.82^{bc}	32.78 ± 0.35^{ef}	0.11 ± 0.05^{a}
LPI-3	19.83 ± 1.32^{abc}	22.08 ± 0.27^{bcd}	14.47 ± 0.30^{ab}	9.36 ± 1.37^{abc}	34.05 ± 0.80^{f}	0.05 ± 0.03^{a}
WPI-3	16.78 ± 2.13^{a}	24.37 ± 0.17^{de}	12.05 ± 1.56^{a}	8.16 ± 0.64^{ab}	38.58 ± 3.22^{g}	0.04 ± 0.03^{a}
SPI-5	19.34 ± 1.36^{ab}	21.25 ± 0.29^{abcd}	16.23 ± 0.32^{bc}	11.13 ± 2.65^{bc}	32.00 ± 3.44^{ef}	0.05 ± 0.04^{a}
LPI-5	21.82 ± 0.90^{bcd}	23.68 ± 0.18^{cde}	18.03 ± 0.42^{cd}	11.86 ± 0.78^{c}	24.54 ± 0.34^{bc}	0.07 ± 0.02^{a}
WPI-5	18.93 ± 0.87^{ab}	26.47 ± 2.71^{e}	18.47 ± 2.60^{cd}	5.91 ± 0.05^{a}	30.16 ± 0.84^{def}	0.07 ± 0.02^{a}
SPI-7	26.55 ± 0.40^{ef}	20.55 ± 2.26^{abc}	18.95 ± 0.86^{cde}	8.43 ± 0.76^{abc}	25.46 ± 1.78^{bcd}	0.05 ± 0.01^{a}
LPI-7	23.61 ± 1.07^{cde}	18.19 ± 0.96^{a}	20.55 ± 0.93^{def}	9.17 ± 2.97^{abc}	28.38 ± 1.88^{cde}	0.11 ± 0.04^{a}
WPI-7	29.20 ± 0.11^{fg}	19.67 ± 0.34^{ab}	22.07 ± 0.23^{f}	6.68 ± 0.09^{a}	22.26 ± 0.16^{b}	0.11 ± 0.03^{a}
SPI-9	30.99 ± 3.67^{g}	24.24 ± 0.69^{de}	19.42 ± 1.90^{def}	7.94 ± 0.59^{ab}	17.34 ± 1.65^{a}	0.07 ± 0.03^{a}
LPI-9	26.30 ± 2.63^{ef}	17.81 ± 2.18^{a}	21.52 ± 0.92^{ef}	7.10 ± 0.12^{a}	26.93 ± 3.66^{bcd}	0.33 ± 0.12^{b}
WPI-9	25.00 ± 1.84^{de}	20.41 ± 2.70^{abc}	19.45 ± 0.65^{def}	8.76 ± 1.89^{abc}	26.36 ± 2.00^{bcd}	0.02 ± 0.02^{a}

Names of samples with numbers indicate the protein isolate gels obtained at the corresponding pH conditions. Significant different ($p \leq 0.05$) among protein gels was denoted by different letters.

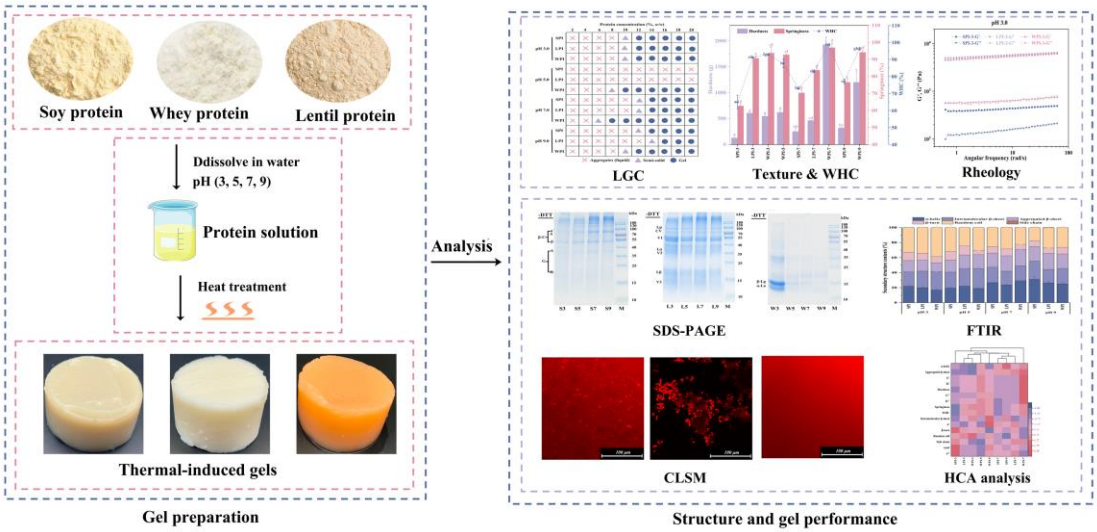

Graphical abstract

Fig. 1. Phase-like diagram of the sol-gel transition of thermal-induced SPI, LPI, and WPI plotted as function of protein concentration and pH.

Fig. 2. Frequency sweep profiles of thermal-induced SPI, LPI, and WPI gels as a function of pH. Names of samples with numbers indicate the protein isolate gels obtained at the corresponding pH conditions.

Fig. 3. SDS-profiles of thermal-induced SPI, LPI and WPI gel fractions as under NR and R conditions a function of pH. M: standard protein markers. S, L, and W mean soy, lentil, and whey protein isolates, respectively. Names of samples with numbers denote the protein isolate gels obtained at the corresponding pH conditions. (a) and (b) mean SPI gels under NR and R conditions, (c) and (d) mean LPI gels under NR and R conditions, (e) and (f) mean WPI gels under NR and R conditions, respectively. Lp: Lipoxygenase; CV: convicilin polypeptides; β-C: β-conglycinin (α, α', β-conglycinin polypeptides); V1-3: vicilin polypeptides; G: glycinin (A: acidic subunit; B: basic subunit); Lα: legumin acidic subunit; Lβ: legumin basic subunit; β-LG: β-lactoglobulin; α-LA: α-lactalbumin; DTT: dithiothreitol).

Fig. 4. Second derivative profile of Amide I region of thermal-induced SPI, LPI, and WPI gels as a function of pH. Names of samples with numbers indicate the protein isolate gels obtained at the corresponding pH conditions.

Fig. 5. Appearance (a) and color values (b) of thermal-induced SPI, LPI, and WPI gels as a function of pH. Names of samples with numbers indicate the protein isolate gels obtained at the corresponding pH conditions. Significant different ($p \leq 0.05$) among protein gels was denoted by different letters.

Fig. 6. CLSM analysis of thermal-induced SPI, LPI, and WPI gels as a function of pH. Names of samples with numbers indicate the protein isolate gels obtained at the corresponding pH conditions.

Fig. 7. Hierarchical cluster analysis of thermal-induced SPI, LPI, and WPI gels as a function of pH. Names of samples with numbers indicate the protein isolate gels obtained at the corresponding pH conditions.

Fig. 1.

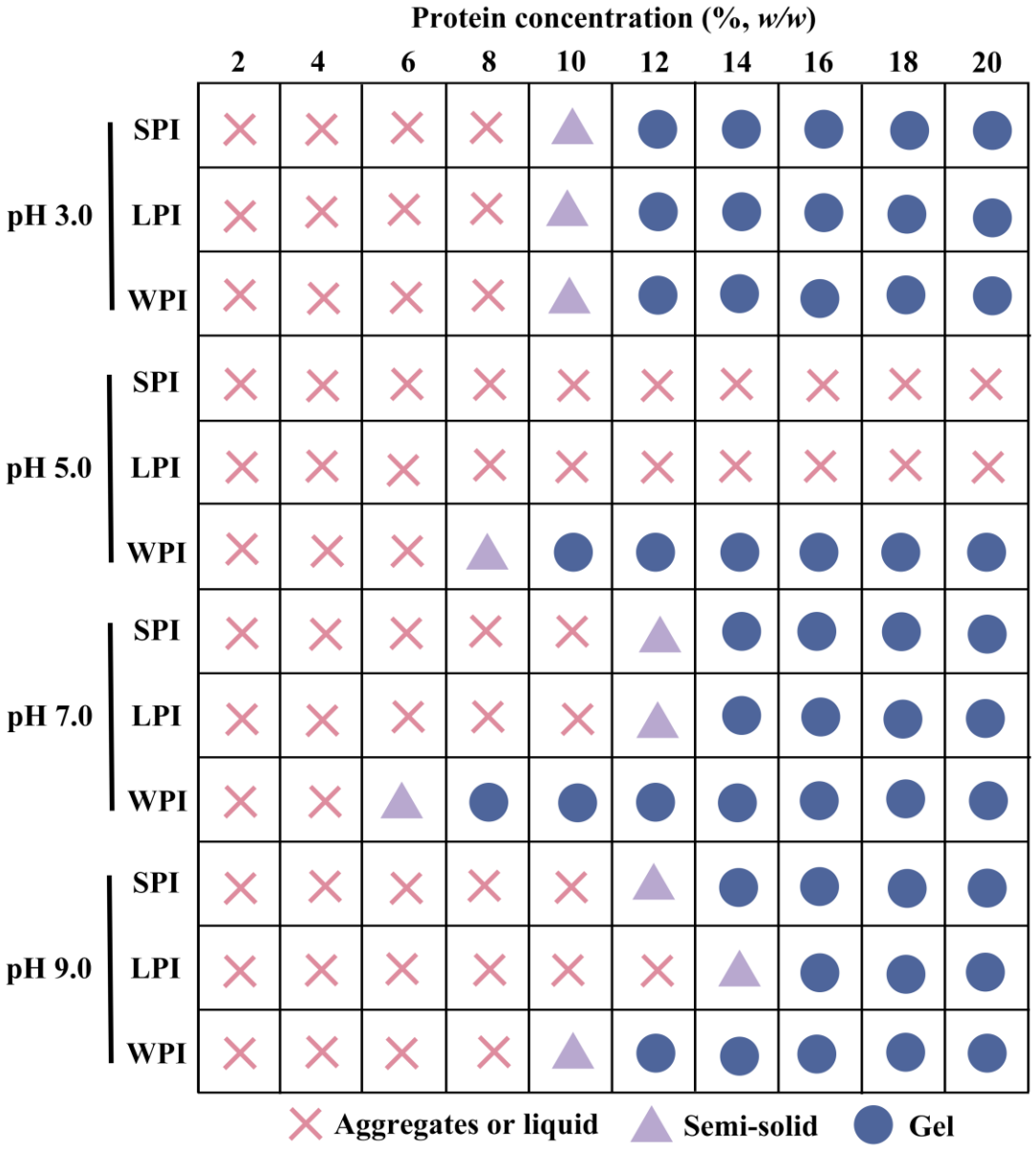
Protein concentration (%, w/w)
2
4
6
8
10
12
14
16
18
20
pH 3.0
pH 5.0
pH 7.0
pH 9.0
SPI
LPI
WPI
Aggregates or liquid
Semi-solid
Gel

Fig. 2.

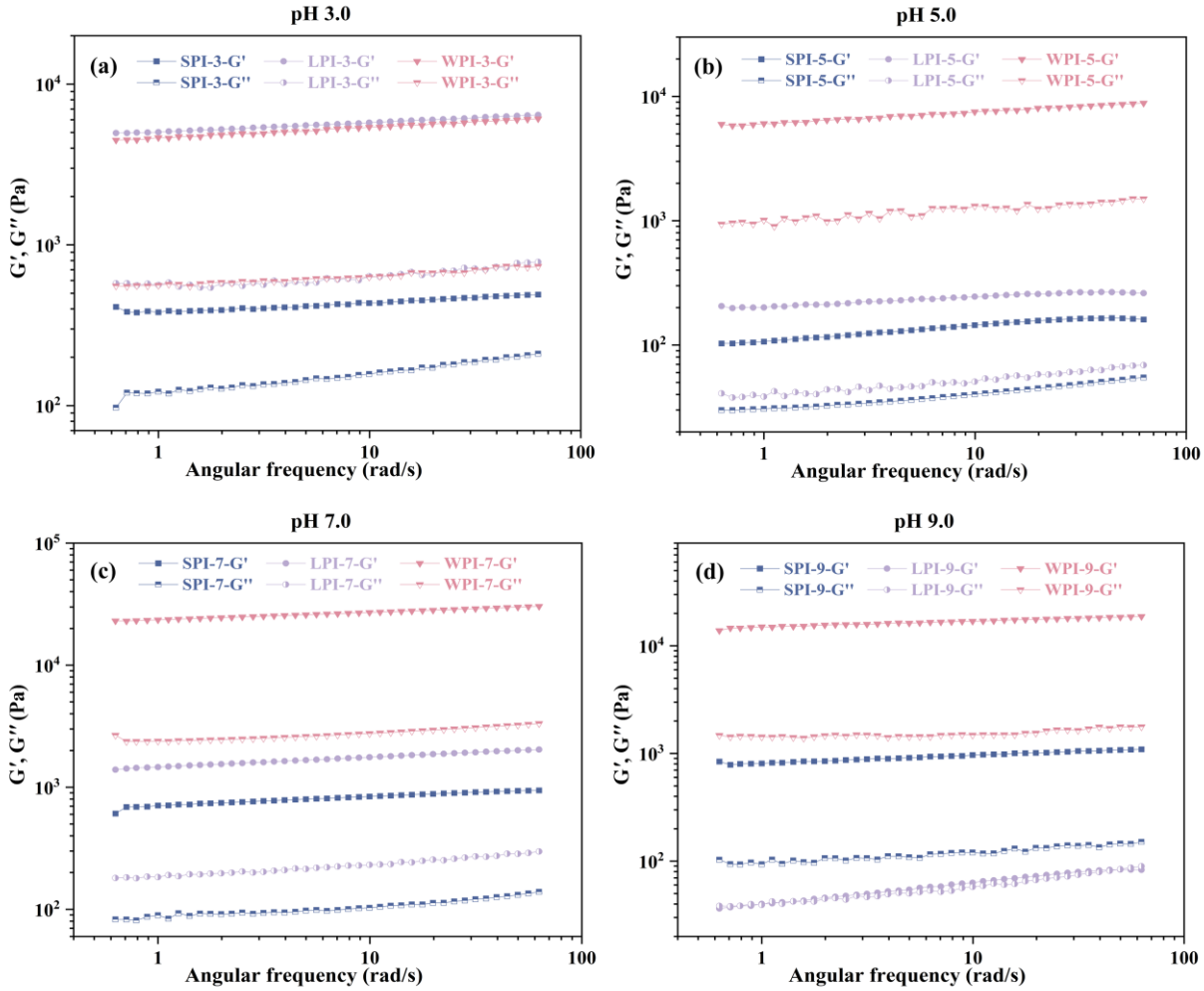
pH 3.0
(a)
SPI-3-G'
SPI-3-G''
LPI-3-G'
LPI-3-G''
WPI-3-G'
WPI-3-G''
G', G'' (Pa)
Angular frequency (rad/s)
pH 5.0
(b)
SPI-5-G'
SPI-5-G''
LPI-5-G'
LPI-5-G''
WPI-5-G'
WPI-5-G''
G', G'' (Pa)
Angular frequency (rad/s)
pH 7.0
(c)
SPI-7-G'
SPI-7-G''
LPI-7-G'
LPI-7-G''
WPI-7-G'
WPI-7-G''
G', G'' (Pa)
Angular frequency (rad/s)
pH 9.0
(d)
SPI-9-G'
SPI-9-G''
LPI-9-G'
LPI-9-G''
WPI-9-G'
WPI-9-G''
G', G'' (Pa)
Angular frequency (rad/s)

Fig. 3.

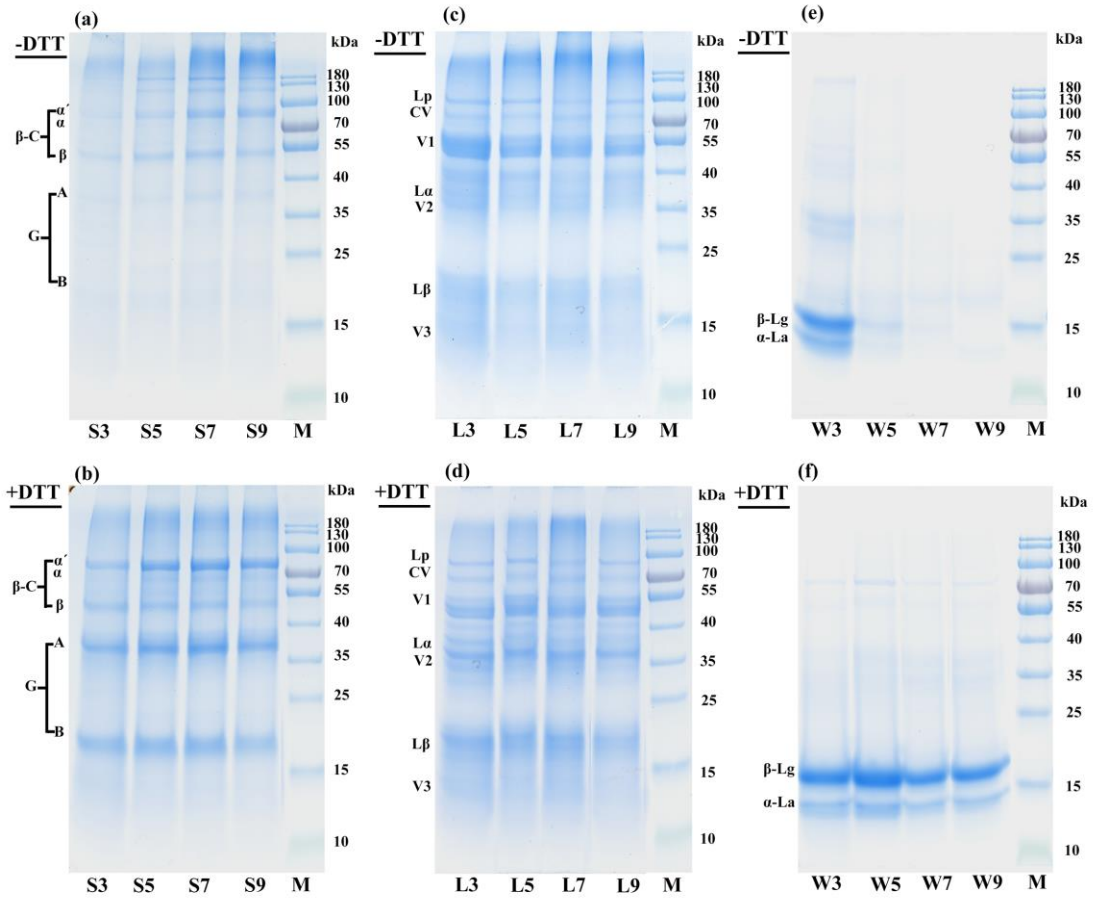
(a)
-DTT
kDa
180
130
100
70
55
40
35
25
15
10
β-C
α´
α
β
G
A
B
S3 S5 S7 S9 M
(c)
-DTT
Lp
CV
V1
Lα
V2
Lβ
V3
L3 L5 L7 L9 M
(e)
-DTT
β-Lg
α-La
W3 W5 W7 W9 M
(b)
+DTT
S3 S5 S7 S9 M
(d)
+DTT
L3 L5 L7 L9 M
(f)
+DTT
W3 W5 W7 W9 M

Fig. 4.

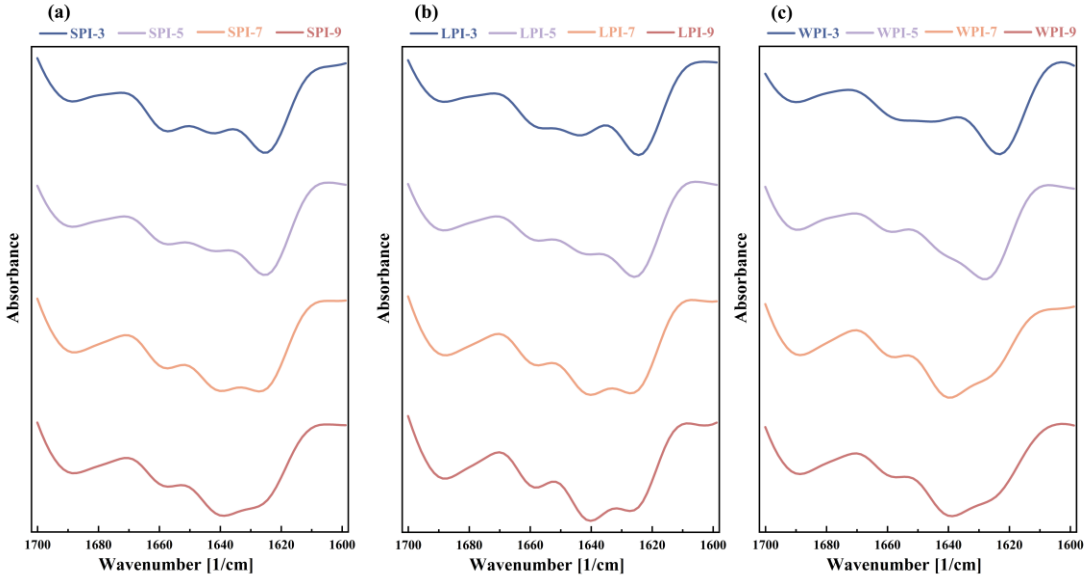
(a)
SPI-3
SPI-5
SPI-7
SPI-9
Absorbance
1700
1680
1660
1640
1620
1600
Wavenumber [1/cm]
(b)
LPI-3
LPI-5
LPI-7
LPI-9
Absorbance
1700
1680
1660
1640
1620
1600
Wavenumber [1/cm]
(c)
WPI-3
WPI-5
WPI-7
WPI-9
Absorbance
1700
1680
1660
1640
1620
1600
Wavenumber [1/cm]

Fig. 5.

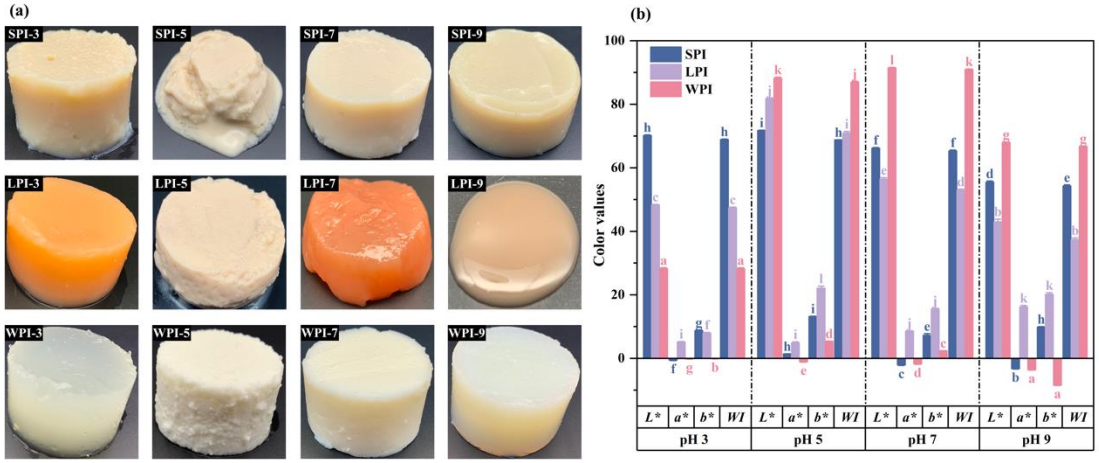
(a)
SPI-3
SPI-5
SPI-7
SPI-9
LPI-3
LPI-5
LPI-7
LPI-9
WPI-3
WPI-5
WPI-7
WPI-9
(b)
SPI
LPI
WPI
Color values
100
80
60
40
20
0
L*
a*
b*
WI
pH 3
pH 5
pH 7
pH 9

Fig. 6.

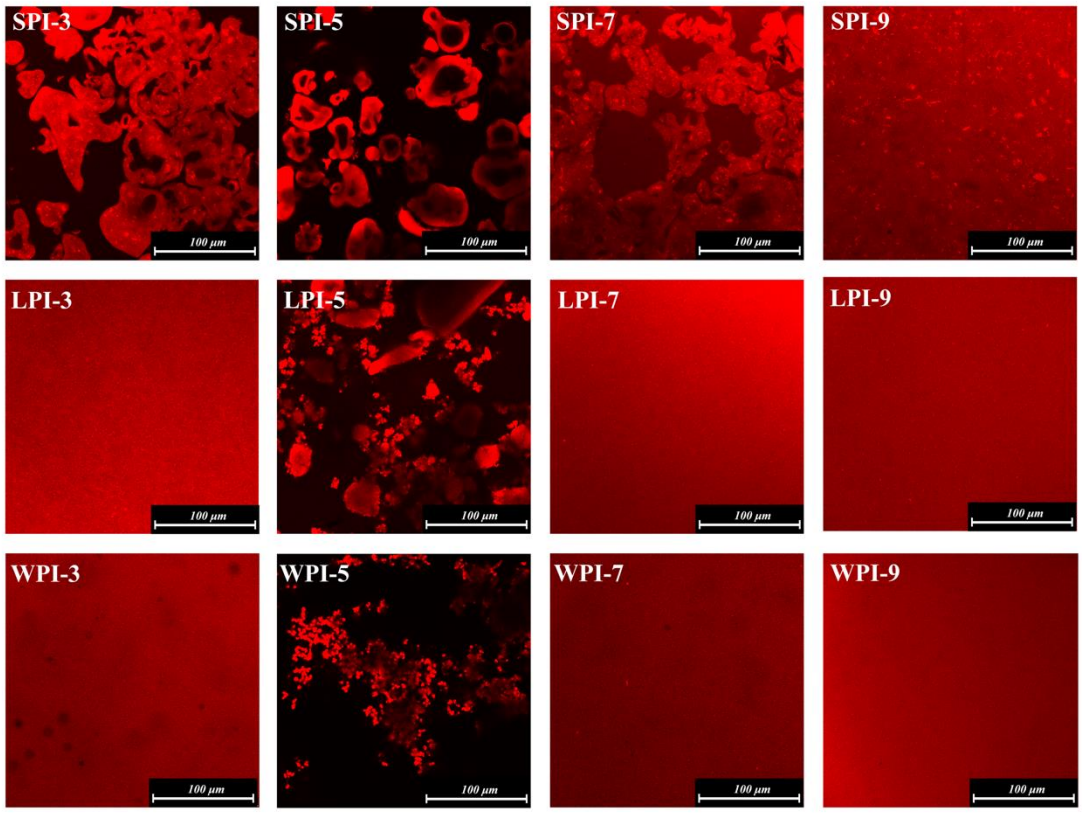
SPI-3
SPI-5
SPI-7
SPI-9
LPI-3
LPI-5
LPI-7
LPI-9
WPI-3
WPI-5
WPI-7
WPI-9
100 μm

953

Fig. 7.

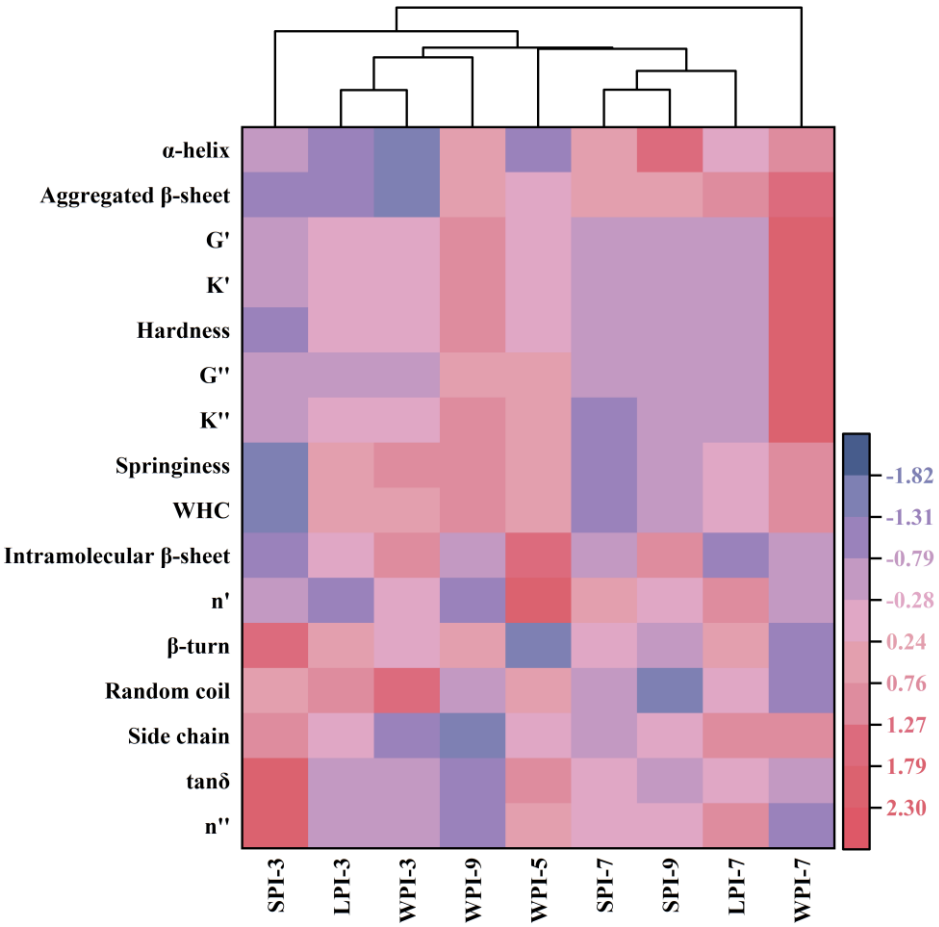
α-helix
Aggregated β-sheet
G'
K'
Hardness
G''
K''
Springiness
WHC
Intramolecular β-sheet
n'
β-turn
Random coil
Side chain
tanδ
n''
SPI-3
LPI-3
WPI-3
WPI-9
WPI-5
SPI-7
SPI-9
LPI-7
WPI-7
-1.82
-1.31
-0.79
-0.28
0.24
0.76
1.27
1.79
2.30

954